Brazilian Journal of Physics (2023) 53:122
https://doi.org/10.1007/s13538-023-01334-5

SBF SOCIEDADE BRASILEIRA DE FÍSICA

GENERAL AND APPLIED PHYSICS

Effect of Perfect Electromagnetic Conductor Wall on the Injected Electron Dynamics in Magnetized Plasma Filled Circular and Elliptical Waveguides

A. Abdoli-Arani[1]

Received: 27 April 2023 / Accepted: 19 June 2023 / Published online: 6 July 2023

Abstract
In the present work, electromagnetic waves propagation in elliptical and circular waveguides filled with a magnetized plasma core and an outer perfect electromagnetic conductor boundary are presented. The components of electromagnetic fields and the power flux density in the considered waveguides are presented. The dispersion relations for the hybrid modes are calculated considering appropriate boundary conditions. The effect of a perfect electromagnetic conductor boundary on the energy and dynamics of an injected electron in the two considered structures is graphically investigated.

Keywords Perfect electromagnetic conductor · Perfect magnetic conductor · Elliptical waveguide · Electromagnetic power flux · Acceleration · Magnetized plasma

1 Introduction

The perfect electromagnetic conductor (PEMC) [1, 2] is the generalization of a perfect electric conductor (PEC) and perfect magnetic conductor (PMC) [3]. Electromagnetic energy and power cannot enter into the PEMC medium because the real values of the admittance M, the complex Poynting vector becomes imaginary [4–6]. The boundary conditions at the surface of the PEMC are expressed in the forms [2]:

$$\hat{n} \times (\vec{H} + M\vec{E}) = 0$$

$$\hat{n} \cdot (\vec{D} - M\vec{B}) = 0$$

where M is the admittance parameter, and it determines the PEMC. In the limits $M = 0$ and $M \to \pm\infty$, the PEMC converts to PMC and PEC, respectively.

Waveguides with different materials have different applications in terahertz, microwave, millimeter, and light waves. Depending on the application of the waveguide, they have different cross-sections and are filled with different materials. Waveguides with PEMC boundaries are of particular importance in the field of wave propagation description [7–9]. A lot of research has been done on the use of PEMC materials [10–12]. Much research has been performed by researchers on particulate acceleration and electron dynamics in the different types of waveguides with various cross-sections and different materials, considering various effects. Some researchers have investigated the acceleration and dynamics of electrons with different EM modes of microwave propagation inside elliptical, circular, and rectangular waveguides containing cold plasma, warm plasma, magnetized plasma, collision plasma, collisionless plasma, homogeneous plasma, inhomogeneous plasma, etc. [13–27].

It is mentioned that PMC boundaries ensure two useful and interesting features. First, PMC cannot allow EM waves and currents to enter the surface. Second, PMC surfaces have a very high surface impedance in a certain limited frequency range, and PMC surfaces reflect EM waves without phase change of the electric field [28].

In the present work, we study wave propagation in the elliptical and circular waveguides filled with a magnetized plasma core and a PEMC boundary as a wall.

We investigate the effect of the PEMC boundary on the EM field propagation and the power flux density in the mentioned waveguides. We investigate the effect of the PEMC boundary on the energy and dynamics of an injected electron in elliptical

✉ A. Abdoli-Arani
abdoliabbas@kashanu.ac.ir

1 Department of Laser and Photonics, Faculty of Physics, University of Kashan, Kashan, Islamic Republic of Iran

and circular waveguides filled with magnetized plasma. We calculate the dispersion functions applied to get the modes.

The present paper is formed into four sections, of which Sect. 1 is the Introduction. Section 2 deals with the calculation of the fields and power flux, and also the dispersion relation, of the hibrid modes in an elliptical waveguide filled by magnetized plasma (MPEW): magnetized plasma elliptical waveguide, core, and a cover PEMC boundary, considering the appropriate boundary conditions. The results are plotted. The effect of the PEMC boundary on the energy and trajectory of an injected electron in the considered configuration is investigated. In Sect. 3, we investigate the fields and power flux, and also the dispersion relation, of the hybrid modes in a circular waveguide filled by magnetized plasma (MPCW): magnetized plasma circular waveguide, core, and a cover PEMC boundary, considering the appropriate boundary conditions. The results are plotted. The effect of the PEMC boundary on the energy and dynamics of an injected electron in the considered configuration is investigated. Finally, the conclusion is stated in Sect. 4.

2 Investigation of the Effect of PEMC Wall in the MPEW Coated with a PEMC

We consider an MPEW coated with a PEMC. An elliptical boundary bounds the plasma, indicated by $\zeta = \zeta_0$, and the plasma is in the constant magnetic field $\vec{B} = B_0\hat{z}$.

Elliptical coordinates are indicated by (ζ, ϑ, z) and are expressed as [29]

$$x = l\cosh\zeta\cos\vartheta \ , \quad y = l\sinh\zeta\sin\vartheta \ , \quad z = z, \tag{1}$$

where $l = \sqrt{a_{xB}^2 - a_{yB}^2}$ is the semi-focal length, a_{xB} and a_{yB} are defined as the semi-major and minor axes of the boundary with ellipse form, and the boundary is indicated by $\zeta_B = arctanh(a_{yB}/a_{xB})$.

The wave equations for E_z and H_z are calculated as

$$\left[\nabla_T^4 + \varsigma 1\nabla_T^2 + \varsigma_2\right]\begin{pmatrix} E_z(\zeta,\vartheta) \\ H_z(\zeta,\vartheta)\end{pmatrix} = 0 \tag{2}$$

where

$$\varsigma_1 = -\frac{\beta^2\varepsilon_P}{\varepsilon_T} + \frac{\omega^2\varepsilon_P}{c^2} + \frac{\omega^2}{c^2}\frac{\varepsilon_T^2 - g^2}{\varepsilon_T} - \beta^2 \tag{3}$$

$$\varsigma_2 = (-\frac{\beta^2\varepsilon_P}{\varepsilon_T} + \frac{\omega^2\varepsilon_P}{c^2})(\frac{\omega^2}{c^2}\frac{\varepsilon_T^2 - g^2}{\varepsilon_T} - \beta^2) - \frac{g^2\varepsilon_P\beta^2\omega^2}{c^2\varepsilon_T^2} \tag{4}$$

$$\nabla_T = \frac{1}{h^2}\frac{\partial^2}{\partial\zeta^2} + \frac{1}{h^2}\frac{\partial^2}{\partial\vartheta^2} \tag{5}$$

Here, $h = l\sqrt{cosh^2\xi - cos^2\eta}$, and β is the axial component of the wave number vector of the propagating wave. Furthermore, the dielectric tensor $\tilde{\varepsilon}$ of the magnetized plasma is indicated as

$$\tilde{\varepsilon} = \begin{pmatrix} \varepsilon_T & ig & 0 \\ -ig & \varepsilon_T & 0 \\ 0 & 0 & \varepsilon_P \end{pmatrix} \tag{6}$$

where g, ε_T, and ε_P are defined as follows:

$$\varepsilon_T = 1 - \frac{\omega_p^2}{\omega^2 - \omega_c^2} \ , \ g = -\frac{\omega_p^2\omega_c}{\omega(\omega^2 - \omega_c^2)} \ , \ \varepsilon_P = 1 - \frac{\omega_p^2}{\omega^2} \tag{7}$$

Here, $\omega_p = (n_0e^2/m_e\varepsilon_0)^{\frac{1}{2}}$ and $\omega_c = eB_0/m_e$ are defined as the electron plasma and cyclotron frequencies, respectively.

The EM fields can be written in the form of transverse and longitudinal components as

$$\vec{E} = \vec{E}_T + \hat{e}_z E_z \tag{8}$$

$$\vec{H} = \vec{H}_T + \hat{e}_z H_z \tag{9}$$

We consider the longitudinal and transverse filed components for the hybrid mode in the magnetized plasma region as

$$\begin{aligned} E_z(\zeta,\vartheta,z,t) = \sum_{m=0}^{\infty}&[C_{1m}Ce_m(\zeta,q_1)ce_m(\vartheta,q_1) \\ &+ C_{2m}Ce_m(\zeta,q_2)ce_m(\vartheta,q_2)]e^{i(\omega t - \beta z + \delta)}, \end{aligned} \tag{10}$$

$$\begin{aligned} H_z(\zeta,\vartheta,z,t) = \sum_{m=0}^{\infty}&-i[h_1C_{1m}Ce_m(\zeta,q_1)ce_m(\vartheta,q_1) \\ &+ h_2C_{2m}Ce_m(\zeta,q_2)ce_m(\vartheta,q_2)]e^{i(\omega t - \beta z + \delta)}, \end{aligned} \tag{11}$$

$$\begin{pmatrix} E_\zeta(\zeta,\vartheta) \\ E_\vartheta(\zeta,\vartheta) \\ H_\zeta(\zeta,\vartheta) \\ H_\vartheta(\zeta,\vartheta) \end{pmatrix} = \begin{pmatrix} \varrho_{11} & \varrho_{12} & \varrho_{13} & \varrho_{14} \\ \varrho_{21} & \varrho_{22} & \varrho_{23} & \varrho_{24} \\ \varrho_{31} & \varrho_{32} & \varrho_{33} & \varrho_{34} \\ \varrho_{41} & \varrho_{42} & \varrho_{43} & \varrho_{44} \end{pmatrix}\begin{pmatrix} \frac{1}{h}\frac{\partial H_z(\zeta,\vartheta)}{\partial\zeta} \\ \frac{1}{h}\frac{\partial H_z(\zeta,\vartheta)}{\partial\vartheta} \\ \frac{1}{h}\frac{\partial E_z(\zeta,\vartheta)}{\partial\zeta} \\ \frac{1}{h}\frac{\partial E_z(\zeta,\vartheta)}{\partial\vartheta} \end{pmatrix} \tag{12}$$

where C_{1m} and C_{2m} are constants, and so $Ce_m(\vartheta, q_i)$ and $Ce_m(\zeta, q_i)$ are defined as the even solutions of the angular and radial Mathieu equations [29]. Furthermore,

$$\varrho_{11} = \frac{\omega^3}{c^2}\mu_0 g\chi_2 \ , \ \varrho_{12} = -i\omega\mu_0\chi_1\chi_2 \ , \tag{13}$$

$$\varrho_{13} = -i\beta\chi_1\chi_2 \ , \ \varrho_{14} = -\frac{\omega^2}{c^2}\beta g\chi_2 \ ,$$

$$\varrho_{21} = i\omega\mu_0 g\chi_1\chi_2 \ , \ \ \varrho_{22} = \frac{\omega^3}{c^2}\mu_0 g\chi_2 \ ,$$

$$\varrho_{23} = \frac{\omega^2}{c^2}\beta g\chi_2 \ , \ \ \varrho_{24} = -i\beta\chi_1\chi_2 \ ,$$

$$\varrho_{31} = -i\beta\chi_1\chi_2 \ , \ \ \varrho_{32} = -\frac{\omega^2}{c^2}g\chi_2 \ , \tag{14}$$

$$\varrho_{33} = -\frac{\omega\beta^2}{\mu_0 c^2}g\chi_2 \ , \ \ \varrho_{34} = \frac{i}{\omega\mu_0}\chi_3\chi_2 \ ,$$

$$\varrho_{41} = \frac{\omega^2}{c^2}\beta\chi_2 \ , \ \ \varrho_{42} = -i\beta\chi_1\chi_2 \ ,$$

$$\varrho_{43} = -i\frac{1}{\mu_0 c^2}\chi_3\chi_2 \ , \ \ \varrho_{44} = -\frac{\omega\beta^2}{\mu_0}g\chi_2 \ ,$$

where

$$\chi_1 = -\beta^2 + \frac{\omega^2\varepsilon_T}{c^2} \ , \ \ \chi_2 = \frac{1}{\chi_1^2 - \frac{g^2\omega^4}{c^4}} \ , \ \ \chi_3 = \chi_1\frac{\omega^2\varepsilon_T}{c^2} - \frac{\omega^4 g^2}{c^4}, \tag{15}$$

and also

$$\iota_{1,2}^2 = \frac{1}{2\varepsilon_T}\left[-(\varepsilon_T + \varepsilon_P)\beta^2 + \frac{\omega^2}{c^2}(\varepsilon_T\varepsilon_P + \varepsilon_T^2 - g^2)\right] \tag{16}$$

$$\pm\frac{1}{2\varepsilon_T}\left\{\left[-(\varepsilon_P - \varepsilon_T)\beta^2 + \frac{\omega^2}{c^2}(\varepsilon_T\varepsilon_P - \varepsilon_T^2 + g^2)\right]^2 + \frac{4\omega^2\beta^2}{c^2}\varepsilon_T^2\varepsilon_P\right\}^{\frac{1}{2}}$$

$$h_{1,2} = \frac{\varepsilon_T}{\mu_0\omega\beta g}\left(\frac{\omega^2\varepsilon_P}{c^2} - \frac{\beta^2\varepsilon_P}{\varepsilon_T} - p_{1,2}^2\right) \tag{17}$$

where $q_1 = \frac{l^2\iota_1^2}{4}$ and $q_2 = \frac{l^2\iota_2^2}{4}$. In this study we choose $\iota_{1,2}^2 > 0$. It is noted that the frequency-wavenumber plane can be divided into regions in which $\iota_{1,2}^2 > 0$, $\iota_{1,2}^2 < 0$, and $\iota_{1,2}^2$ are complex [30].

2.1 Dispersion Equation

Using the correct and appropriate boundary conditions, the dispersion equation is derived. The PEMC boundary conditions are expressed as [2, 9]

$$H_z|_{\zeta=\zeta_0} + ME_z|_{\zeta=\zeta_0} = 0 \tag{18}$$

$$H_\vartheta|_{\zeta=\zeta_0} + ME_\vartheta|_{\zeta=\zeta_0} = 0 \tag{19}$$

The dispersion equation is derived from the above boundary by setting the condition that the determinant of the coefficients of these equations becomes equal to zero:

$$DR = a_{11}a_{22} - a_{12}a_{21} \tag{20}$$

where

$$\begin{aligned} a_{11} &= T_1 s_1 \ , \\ a_{12} &= T_2 s_2 \ , \\ a_{21} &= (T_3 + T_5)s_1 + (T_4 + T_6)s_3 \ , \\ a_{22} &= (T_7 + T_9)s_2 + (T_8 + T_{10})s_4 \ , \end{aligned} \tag{21}$$

$$\begin{aligned} T_1 &= (-ih_1 + M)Ce_m(\zeta_0, q_1) \ , \\ T_2 &= (-ih_2 + M)Ce_m(\zeta_0, q_2) \ , \end{aligned} \tag{22}$$

$$T_3 = -i(\beta k_0^2 + M\omega\mu_0 k_0^2)g\chi_2 h_1 Ce'_m(\zeta_0, q_1) \ , \tag{23}$$

$$T_4 = -(\beta + M\omega\mu_0)\chi_1\chi_2 h'_1 Ce_m(\zeta_0, q_1) \ , \tag{24}$$

$$T_5 = -i\left(\frac{\chi_3}{\omega\mu_0} + M\beta\chi_1\right)\chi_2 Ce'_m(\zeta_0, q_1) \ , \tag{25}$$

$$T_6 = -\left(\frac{\beta^2 k_0^2}{\omega\mu_0} + M\beta k_0^2\right)g\chi_2 Ce_m(\zeta_0, q_1) \ , \tag{26}$$

$$T_7 = -i(\beta k_0^2 + M\omega\mu_0 k_0^2)g\chi_2 h_2 Ce'_m(\zeta_0, q_2) \ , \tag{27}$$

$$T_8 = -(\beta + M\omega\mu_0)\chi_1\chi_2 h_2 Ce_m(\zeta_0, q_2) \ , \tag{28}$$

$$T_9 = -i\left(\frac{\chi_3}{\omega\mu_0} + M\beta\chi_1\right)\chi_2 Ce'_m(\zeta_0, q_2) \ , \tag{29}$$

$$T_{10} = -\left(\frac{\beta^2 k_0^2}{\omega\mu_0} + M\beta k_0^2\right)g\chi_2 Ce_m(\zeta_0, q_2) \ , \tag{30}$$

and

$$s_1 = \int_0^{2\pi} ce_n(\vartheta, q_1)ce_m(\vartheta, q_1)d\vartheta, \tag{31}$$

$$s_2 = \int_0^{2\pi} ce_n(\vartheta, q_1)ce_m(\vartheta, q_2)d\vartheta, \tag{32}$$

$$s_3 = \int_0^{2\pi} ce_n(\vartheta, q_1)ce'_m(\vartheta, q_1)d\vartheta, \tag{33}$$

$$s_4 = \int_0^{2\pi} ce_n(\vartheta, q_1)ce'_m(\vartheta, q_2)d\vartheta. \quad (34)$$

2.2 Injected Electron Dynamics in the MPEW with PEMC Wall

Now, we study the effect of the PEMC wall on the dynamics of injected electrons in the MPEW. For this aim, we use the Lorentz and energy equations for electrons:

$$\frac{d(\gamma m_e v_x)}{dt} = -e[E_x + v_y B_z + v_y B_0 - v_z B_y], \quad (35)$$

$$\frac{d(\gamma m_e v_y)}{dt} = -e[E_y + v_z B_x - v_x B_z - v_x B_0)], \quad (36)$$

$$\frac{d(\gamma m_e v_z)}{dt} = -e[E_z + v_x B_u - v_y B_x], \quad (37)$$

and

$$\frac{d(\gamma m_e c^2)}{dt} = -e(v_x E_x + v_y E_y + v_z E_z), \quad (38)$$

$-e$ is the electron charge and m_e is the rest mass of the electron. We solve the above equations by the fourth-order Runge–Kutta method.

For numerical investigation, we consider that an electron with an initial energy of $20\ keV$ is injected into the waveguide with plasma density $\sim 10^{17} m^{-3}$, and assume $m = 1, n = 1$.

In Fig. 1, we plotted dispersion curves for different values of the PEMC admittance parameter, M , in the MPEW coated with a PEMC. Figure 2 shows the variation of the power flux density versus ζ and ϑ in the MPEW coated with a PEMC. The power flux density can be calculated as follows: $S_z = \frac{1}{2}Re(E_\zeta H_\vartheta^* - E_\vartheta H_\zeta^*)$.

In Fig. 3, we plotted the three-dimensional trajectory of the electron in the MPEW coated with a PEMC, for different values of the M parameter. We considered $M_1 = 0.002$, $M_2 = 0.006$, and $M_3 = 0.01$.

Figure 4 illustrates the energy of the electron in the MPEW coated with a PEMC for different values of the M parameter. We considered $M_1 = 0.002$, $M_2 = 0.01$, and $M_3 = 0.1$.

3 Investigation of the Effect of PEMC Wall in the MPCW Coated with a PEMC

The wave equations for E_z and H_z are obtained as the following forms:

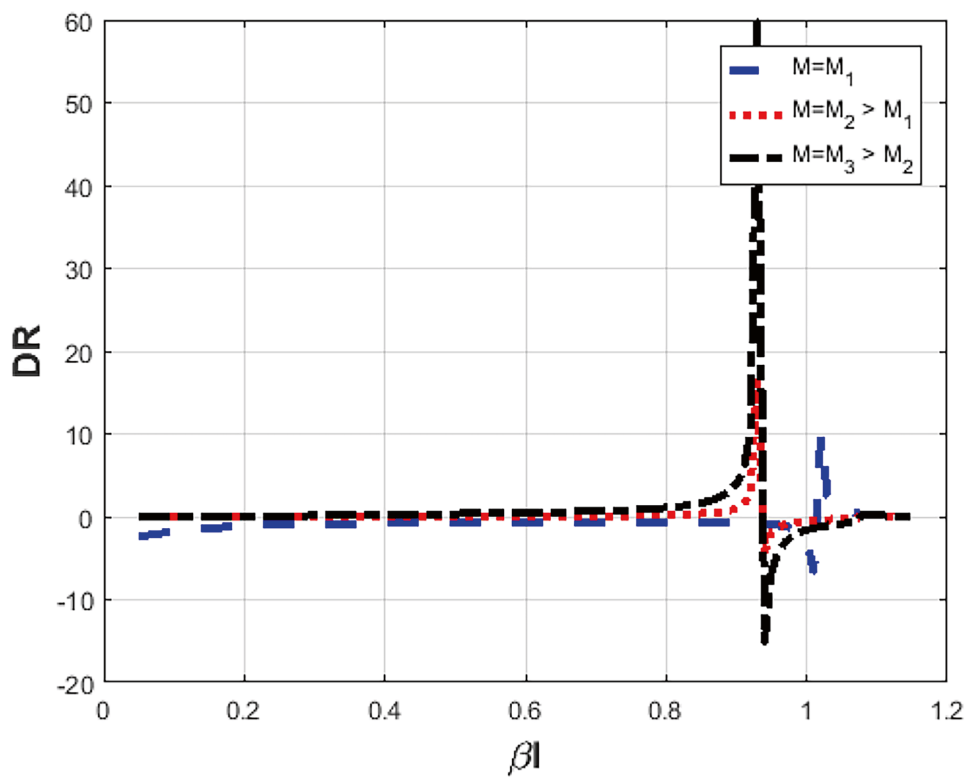

Fig. 1 Plot of DR versus normalized wave number, βl, for different values of M in the MPEW coated with a PEMC

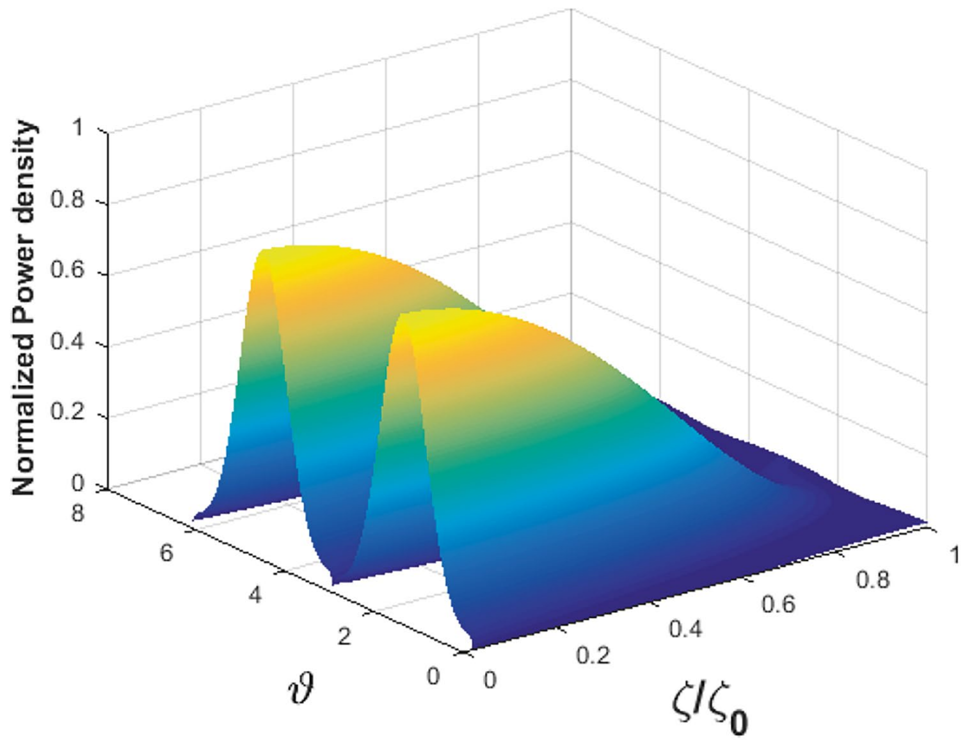

Fig. 2 Plot of the power flux density versus ζ and ϑ in the MPEW coated with a PEMC

$$E_z(\rho,\phi,z,t)=\sum_{m=0}^{\infty}[J_{1m}J_m(p_1\rho)+J_{2m}J_m(p_2\rho)]e^{i(\omega t-\beta z+m\phi+\delta)}, \tag{39}$$

$$H_z(\rho,\phi,z,t)=\sum_{m=0}^{\infty}-i[h_1J_{1m}J_m(p_1\rho)+h_2J_{2m}J_m(p_2\rho)]e^{i(\omega t-\beta z+m\phi+\delta)}, \tag{40}$$

Furthermore, transverse electric and magnetic field components are obtained in the following forms:

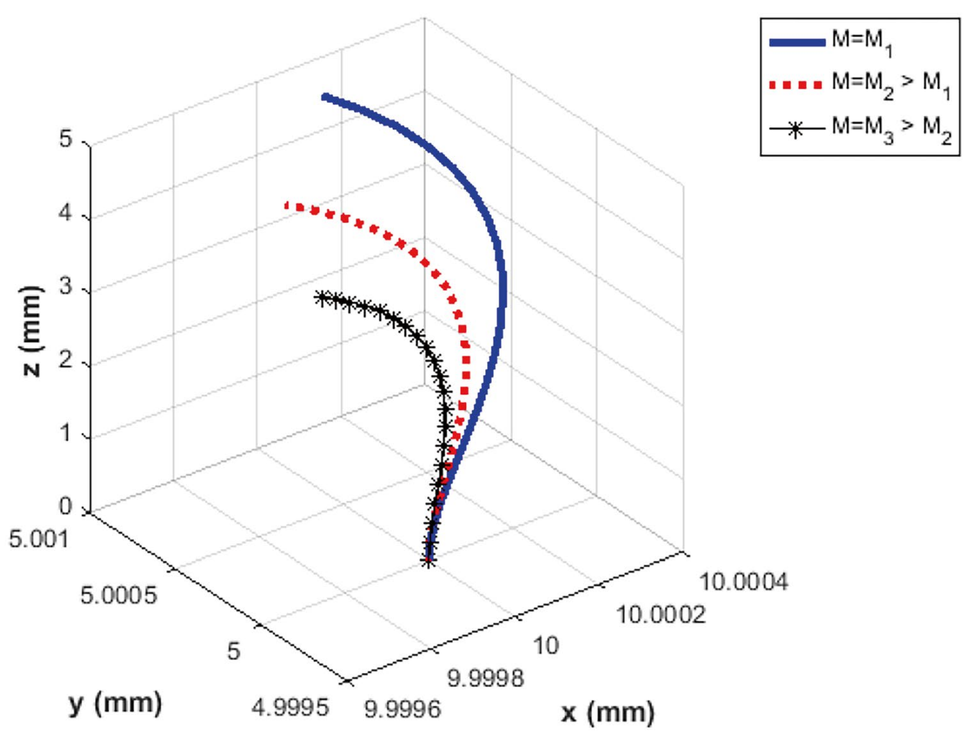

Fig. 3 Electron trajectory for different values of M in the MPEW coated with a PEMC

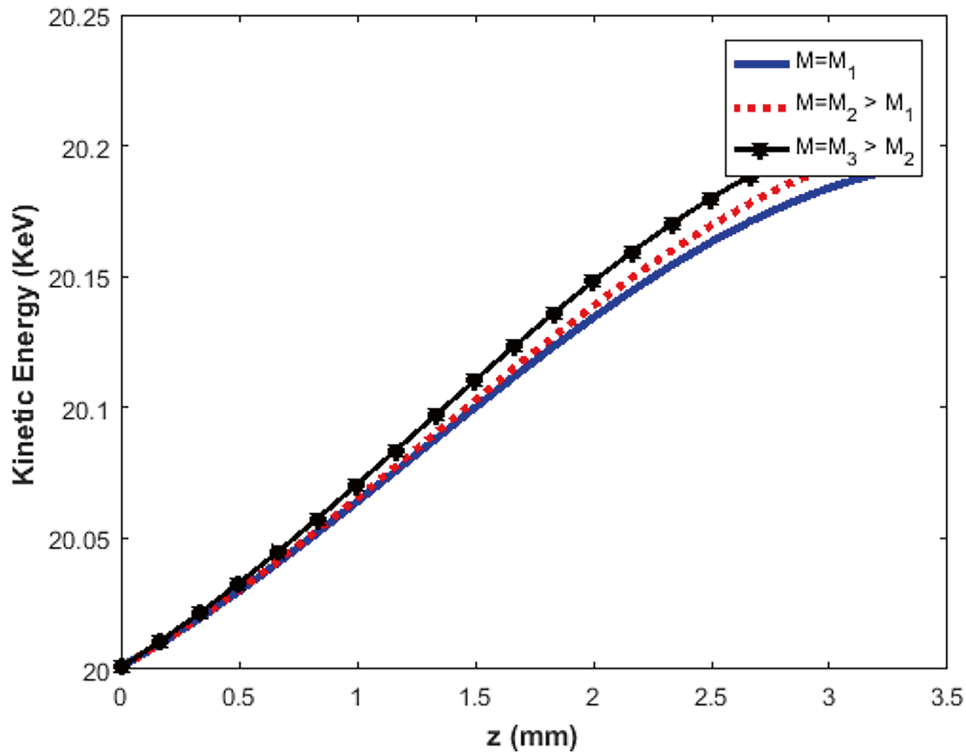

Fig. 4 Electron energy for different values of M in the MPEW coated with a PEMC

$$\begin{pmatrix} E_\rho(\rho,\phi) \\ E_\phi(\rho,\phi) \\ H_\rho(\rho,\phi) \\ H_\phi(\rho,\phi) \end{pmatrix} = \begin{pmatrix} \varrho_{11} & \varrho_{12} & \varrho_{13} & \varrho_{14} \\ \varrho_{21} & \varrho_{22} & \varrho_{23} & \varrho_{24} \\ \varrho_{31} & \varrho_{32} & \varrho_{33} & \varrho_{34} \\ \varrho_{41} & \varrho_{42} & \varrho_{43} & \varrho_{44} \end{pmatrix} \begin{pmatrix} \frac{\partial H_z(\rho,\phi)}{\partial \rho} \\ \frac{1}{\rho}\frac{\partial H_z(\rho,\phi)}{\partial \phi} \\ \frac{\partial E_z(\rho,\phi)}{\partial \rho} \\ \frac{1}{\rho}\frac{\partial E_z(\rho,\phi)}{\partial \phi} \end{pmatrix} \tag{41}$$

Using the boundary conditions,

$$H_z|_{\rho=\rho_0} + ME_z|_{\rho=\rho_0} = 0 \tag{42}$$

$$H_\phi|_{\rho=\rho_0} + ME_\phi|_{\rho=\rho_0} = 0, \tag{43}$$

we obtain the dispersion relation

$$DR = a_{11}a_{22} - a_{12}a_{21} \tag{44}$$

where we calculate

$$\begin{aligned} a_{11} &= T_1 , \\ a_{12} &= T_2 , \\ a_{21} &= (T_3 + T_5) + (T_4 + T_6)\frac{im}{\rho} , \\ a_{22} &= (T_7 + T_9)s_2 + (T_8 + T_{10})\frac{im}{\rho} , \end{aligned} \tag{45}$$

$$T_1 = (-ih_1' + M)J_m(p_1\rho_0) , \; T_2 = (-ih_2' + M)J_m(p_2\rho_0) , \tag{46}$$

$$T_3 = -i(\beta k_0^2 + M\omega\mu_0 k_0^2)g\chi_2 h_1' J_m'(p_1\rho_0) , \tag{47}$$

$$T_4 = -(\beta + M\omega\mu_0)\chi_1\chi_2 h_1' J_m(p_1\rho_0) , \tag{48}$$

$$T_5 = -i(\frac{\chi_3}{\omega\mu_0} + M\beta\chi_1)\chi_2 J_m'(p_1\rho_0) , \tag{49}$$

$$T_6 = -(\frac{\beta^2 k_0^2}{\omega\mu_0} + M\beta k_0^2)g\chi_2 J_m(p_1\rho_0) , \tag{50}$$

$$T_7 = -i(\beta k_0^2 + M\omega\mu_0 k_0^2)g\chi_2 h_2' J_m'(p_2\rho_0) , \tag{51}$$

$$T_8 = -(\beta + M\omega\mu_0)\chi_1\chi_2 h_2' J_m(p_2\rho_0)) , \tag{52}$$

$$T_9 = -i(\frac{\chi_3}{\omega\mu_0} + M\beta\chi_1)\chi_2 J_m'(p_2\rho_0) , \tag{53}$$

$$T_{10} = -(\frac{\beta^2 k_0^2}{\omega\mu_0} + M\beta k_0^2)g\chi_2 J_m(p_2\rho_0) . \tag{54}$$

For numerical investigation, similar to the previous section, we calculate and plot the obtained results in the MPCW coated with a PEMC.

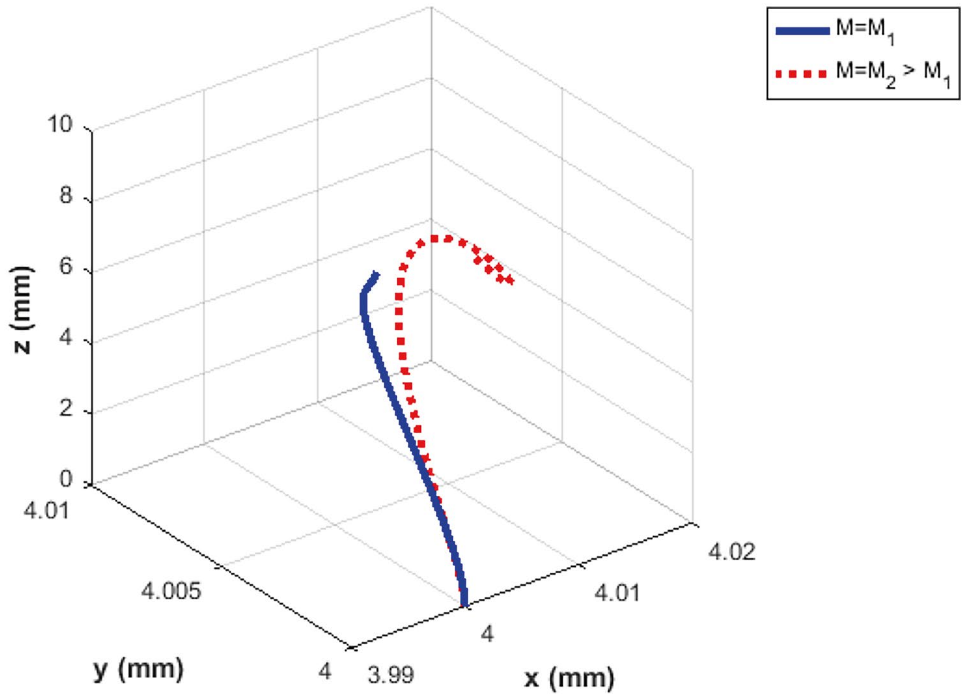

Fig. 5 Electron trajectory for different values of M in the MPCW coated with a PEMC

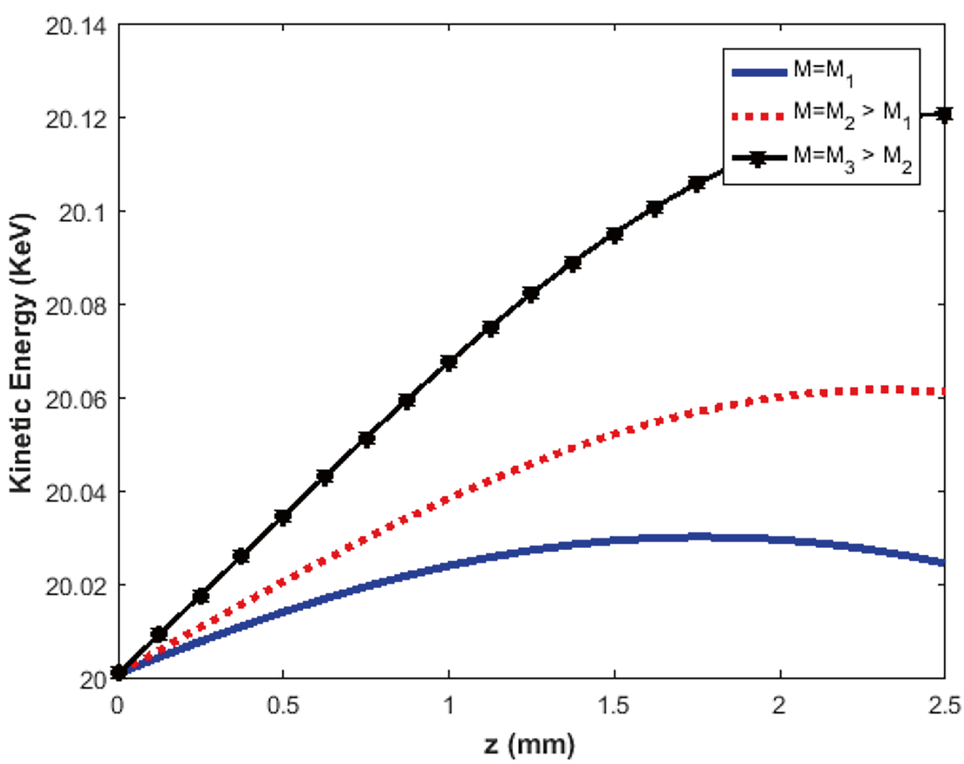

Fig. 6 Electron energy for different values of M in the MPCW coated with a PEMC

In Fig. 5, we plotted the three-dimensional trajectory of the electron in the MPCW coated with a PEMC, for different values of the PEMC admittance parameter. We considered $M_1 = 0.001$ and $M_2 = 0.004$. Figure 6 illustrates the energy of the electron in the MPCW coated with a PEMC, for different values of the M parameter. We considered $M_1 = 0.001$, $M_2 = 0.004$, and $M_3 = 0.01$.

4 Conclusions

In this work, we considered MPEW and MPCW coated with a PEMC boundary as cover. The EM wave propagation in two considered waveguides was studied. Considering appropriate boundary conditions, dispersion relations for the hybrid modes were derived. The EM fields and the power flux density in the mentioned waveguides were presented. The effect of a PEMC boundary on the energy and dynamics of an injected electron in the two considered configurations was graphically studied. In the end, it seems necessary to mention that the obtained results are approximate and in the considered frequency and parameter range. Various effects may appear in practical applications. We omitted some effects. However, the results are good and acceptable.

Author Contribution The author confirms that all authors contributed equally to the paper.

Funding Funding was provided by the University of Kashan, Kashan, Islamic Republic of Iran.

Data Availability The author confirms that the data supporting the findings of this study are available within the article and its supplementary materials.

Declarations

Ethics Approval Not applicable; no experiment has been conducted on human or animals.

Conflict of Interest The author declares no competing interests.

References

1. I.V. Lindell, A.H. Sihvola, Perfect EM conductor. J. Electromag. Waves Appl. **19**, 861–869 (2005)
2. I.V. Lindell, A.H. Sihvola, Realization of the PEMC boundary. IEEE Trans. Anten. Propag. **53**, 3012–3018 (2005)
3. S. Ahmad, Q.A. Naqvi, Electromagnetic scattering from a perfect electromagnetic conductor circular cylinder coated with a metamaterial having negative permittivity and/or permeability. Opt. Commun. **281**, 5664–5670 (2008)
4. M.A. Fiaz, A. Ghaffar, Q.A. Naqvi, High frequency expressions for the field in caustic region of PEMC cylindrical reflector using Maslov's method. J Electromagn. Waves Appl. **22**, 385–397 (2008)
5. A. Ghaffar, M. Yaqoob, M.A. Alkanhal, S. Ahmed, Q. Naqvi, M. Kalyar, Scattering of electromagnetic wave from perfect EM conductor cylinders placed in un-magnetized isotropic plasma medium. Opt. Int. J. Light Electron Opt. **125**, 4779–4783 (2014)
6. A. Ghaffar, M. Yaqoob, M.A. Alkanhal, M. Sharif, Q. Naqvi, Electromagnetic scattering from anisotropic plasma-coated perfect EM conductor cylinders. AEU-Int. J. Electron. Commun. **68**, 767–772 (2014)
7. M. Baqir, P. Choudhury, Dispersion characteristics of optical fibers under PEMC twists. J. Electromagn. Waves Appl. **28**, 2124–2134 (2014)
8. A. Hussain, Q.A. Naqvi, Perfect electromagnetic conductor (PEMC) and fractional waveguide. Prog. Electromagn. Res. **73**, 61–69 (2007)
9. A. Ghaffar, M.A.S. Alkanhal, Power flux distribution in chiro-plasma filled perfect electromagnetic conductor circular waveguides. Radio Sci. **51**, 231–240 (2016)
10. I.V. Lindell, A.H. Sihvola, Realization of the PEMC boundary. Antennas Propag. IEEE Trans. **53**, 3012–3018 (2005)
11. I.V. Lindell, A. Sihvola, The PEMC resonator. J. Electromagn. Waves Appl. **20**, 849–859 (2006)
12. I.V. Lindell, A.H. Sihvola, Losses in the PEMC boundary. Antennas Propag. IEEE Trans. **54**, 2553–2558 (2006)
13. B.F. Mohamed, A.M. Gouda, Electron acceleration by microwave radiation inside a rectangular waveguide. Plasma Sci. Technol. **13**, 357–361 (2011)
14. B.F. Mohamed, A.M. Gouda, L.Z. Ismail, Electron dynamics in presence of static helical magnet inside circular waveguide. IEEE Trans. Plasma Sci. **39**, 842–846 (2011)
15. H.K. Malik, S. Kumar, K.P. Singh, Electron acceleration in a rectangular waveguide filled with unmagnetized inhomogeneous cold plasma. Laser Part. Beams **26**, 197–205 (2008)
16. S.K. Jawla, S. Kumar, H.K. Malik, Evaluation of mode fields in a magnetized plasma waveguide and electron acceleration. Opt. Commun. **251**, 346–360 (2005)
17. D.N. Gupta, N. Kant, D.E. Kim, H. Suk, Electron acceleration to GeV energy by a radially polarized laser. Physics Letter A **368**, 402–407 (2007)
18. M. Litos et al., High-efficiency acceleration of an electron beam in a plasma wakefield accelerator. Nature **515**, 92–95 (2014)
19. L. Xiao, W. Gai, X. Sun, Field analysis of a dielectric-loaded rectangular waveguide accelerating structure. Phys. Rev. E **65**, 016505-1–016505-9 (2002)
20. A. Abdoli-Arani, M.J. Basiry, Influence of electron-ion collisions in plasma on the electron energy gain using the TE11 mode inside an elliptical waveguide. Physica Scripta **91**(9), 095602 (2016)
21. A. Abdoli-Arani, M. Moghaddasi, Study of electron acceleration through the TE11 mode in a collisional plasma-filled cylindrical waveguide. Waves Random Complex Media **26**(3), 339–347 (2016)
22. A. Abdoli-Arani, Electron acceleration considering pondermotive force effect in a plasma-filled rectangular waveguide by microwave radiation. Waves Random Complex Media **26**(4), 407–416 (2016)
23. A. Abdoli-Arani, N. Ghanbari, Nonlinear effect of microwave longitudinal ponderomotive force on the dynamics and energy of an externally injected electron in an inhomogeneous plasma filled circular and elliptical cylinder waveguides. Waves Random Complex Media 1–17 (2019)
24. A. Abdoli-Arani, Electron energy gain in the transverse electric mode of a coaxial waveguide filled with plasma by microwave radiation. Waves Random Complex Media **25**(3), 350–360 (2015)
25. A. Abdoli-Arani, Electron energy gain in the fundamental mode of an elliptical waveguide in the presence of static helical magnet

by microwave radiation. Waves Random Complex Media **25**(2), 243–258 (2015)
26. S. Kumar, M. Yoon, Electron dynamics and acceleration study in a magnetized plasma-filled cylindrical waveguide. J. Appl. Phys. **103**, 023302-1–023302-7 (2008)
27. S. Kumar, M. Yoon, Electron acceleration in a warm magnetized plasma-filled cylindrical waveguide. J. Appl. Phys. **104**, 073303-1–073303-6 (2008)
28. J.R. Sohn, K.Y. Kim, H.-S. Tae, H.J. Lee, Comparative study on various artificial magnetic conductors for low-profile antenna. Prog. Electromagn. Res. **61**, 27–37 (2006)
29. N.W. McLachlan, Theory and Application of Mathieu Functions (Dover, New York, ch. 16, 1964), p. 294
30. S. Ivanov, E. Alexov, Electromagnetic waves in a plasma wave-guide. J. Plasma Phys. **43**(1), 51–67 (1990)